Steady-State Fluorescence Spectroscopy as a Tool to Monitor Protein/Ligand Interactions

3

Roopa Kenoth, Balamurali M. M., and Ravi Kanth Kamlekar

Abstract

Fluorescence spectroscopy is an ideal and powerful methodology for the potent and reliable study of protein–ligand interactions. Enhanced susceptibility accompanied with comparative easiness forms the prominent key factor for the application of fluorescence techniques in these studies. In fluorescence technique, protein–ligand interactions are often studied at very low concentrations compared to other optical methods with a thousandfold higher sensitivity. In this method, we measure the variation in quantum yield upon ligand binding, by observing variations in ligand fluorescence, intrinsic protein fluorescence, or fluorescence of covalently or noncovalently bound fluorescent probes that are sensitive to ligand binding. Sensitivity of a fluorescent ligand to the environment, energy transfer from protein to ligand producing reduction in protein fluorescence or amplification of ligand fluorescence, a conformational change in protein/ ligand on binding to the protein, etc., contribute to the changes in quantum yield upon ligand binding [1–3]. This chapter will outline a sketch of steady-state fluorescence techniques for defining molecular interactions and calculation of binding constants.

R. Kenoth · R. K. Kamlekar (✉)
Department of Chemistry, School of Advanced Sciences, VIT, Vellore, Tamilnadu, India
e-mail: ravikanth.k@vit.ac.in

B. M. M.
Division of Chemistry, School of Advanced Sciences, VIT, Chennai, Tamilnadu, India

H. Sahoo (ed.), *Optical Spectroscopic and Microscopic Techniques*,
https://doi.org/10.1007/978-981-16-4550-1_3

3.1 Introduction

Fluorescence spectroscopy is an ideal and powerful methodology for the potent and reliable study of protein–ligand interactions. Enhanced susceptibility accompanied with comparative easiness forms the prominent key factor for the application of fluorescence techniques in these studies. In fluorescence technique, protein–ligand interactions are often studied at very low concentrations compared to other optical methods with a thousandfold higher sensitivity. In this method, we measure the variation in quantum yield upon ligand binding, by observing variations in ligand fluorescence, intrinsic protein fluorescence, or fluorescence of covalently or noncovalently bound fluorescent probes that are sensitive to ligand binding. Sensitivity of a fluorescent ligand to the environment, energy transfer from protein to ligand producing reduction in protein fluorescence or amplification of ligand fluorescence, a conformational change in protein/ ligand on binding to the protein, etc., contribute to the changes in quantum yield upon ligand binding [1–3]. This chapter will outline a sketch of steady-state fluorescence techniques for defining molecular interactions and calculation of binding constants.

3.1.1 Basic Concepts

Emission and excitation spectra along with quantum yield and anisotropy are the distinguishing features of protein fluorescence. These specifications get altered during the association of a protein with another protein or ligand based on the immediate surroundings of the fluorophore. Therefore, these parameters are regularly used to measure the magnitude of complex formation associated with a particular interaction.

3.1.2 Intrinsic Protein Fluorescence

Intrinsic protein fluorescence is employed to gain knowledge about ligand binding. Intrinsic fluorescence of proteins is contributed largely by aromatic amino acid residues like tryptophan (Trp), tyrosine (Tyr), and phenylalanine (Phe) [4]. The quantum yield and molar extinction coefficient of Trp residues are high in accordant with stronger fluorescence compared to the Tyr and Phe. Energy transfer from Tyr and Phe to Trp is also possible. Protein–ligand interaction often alters the fluorescence of proteins. Information on conformational and structural changes during the interaction with various ligands is derived from the sensitivity of tryptophan residues to the polarity of the immediate environment [4, 5]. Trp residues are mostly found in the binding sites or at the subunit interfaces as they possess a greater tendency to interact through hydrophobic interactions as well as hydrogen bonds. Solvent accessibility and local mobility are often limited by ligand binding. The spectrum will shift to blue with a change in intensity and polarization during this process. Fluorescence intensity decreases if ligand binding leads to conformational change [which brings quenching group in the vicinity of the fluorophore or if the ligand is

close enough to tryptophan(s)]. For most practical applications, Trp residues are excited at 295 nm to avoid contributions from other residues especially Tyr. In a nonpolar environment, Trp residues fluoresce at 320 nm while emission occurs at significantly longer wavelengths in polar surroundings [6].

3.1.3 Extrinsic Fluorescent Probes

Extrinsic fluorescent probes are employed when there is a poor response in intrinsic fluorescence upon protein–ligand interaction [7]. By conjugating these probes to proteins, nucleic acids, or lipids, the sensitivity and quality of the information provided by fluorescence spectrometry can be improved. Hydrophobic fluorescent ligands such as ANS are strongly fluorescent only when bound to the protein. Its derivatives like Prodan and Nile Red are also suitable means to explore protein–ligand interactions. The second category of solvent-sensitive fluorescent probe is Ketocyanines. Competition experiments can be carried out in which other ligands compete with this fluorophore. Thus fluorescence of both intrinsic and extrinsic may therefore be used for estimating dissociation constant (K_d) values of ligand binding with proteins. Fluorescent compounds, such as fluorescein, and rhodamine derivatives in addition to cyanine compounds may be combined with the ligand and employed for studying protein–ligand association. Fluorescence properties of cofactors such as NAD, FAD, and porphyrins are also helpful for in vitro applications [7–9].

3.2 Steady-State Fluorescence Analysis

Steady-state fluorescence is a general method used to measure the binding interactions of proteins. High sensitivity and capacity to execute measurements even in dilute protein solutions are the major advantages of fluorescence studies. The high sensitivity of tryptophan to its surroundings assists to detect protein association reactions by fluorescence. Fluorescence emission maximum or quantum yield of tryptophan residues are altered subjected to a change in solvent or a change in the vicinity of quenching groups [10–12].

The tertiary structure of the protein is often altered during protein–ligand binding. This change could affect the environment of intrinsic or extrinsic fluorophore of the protein, and as a consequence, the fluorescence spectrum gets altered and the changes observed at certain wavelengths may help to calculate the dissociation constant (K_d) of the protein–ligand complex. K_d is an estimate of the attraction of the protein for a particular ligand and is evaluated as shown below in Eq. (3.1).

$$\begin{aligned} &P + L \rightleftarrows PL \\ &K_d = [P][L]/[PL] \end{aligned} \tag{3.1}$$

3.2.1 Fluorescence Analysis of Protein–Ligand/Drug Interactions

Fluorescence titrations are the most commonly used method for studying the protein–ligand interactions provided one can obtain an apparent variation in fluorescence as a result of binding to the ligand (Fig. 3.1). The ratio of protein to the ligand is changed gradually by changing their concentrations generally by sequential dilution during a fluorescence titration. Binding sites get saturated with an increase in the concentration of ligand (Fig. 3.2).

Half the concentration of the ligand at half saturation point is considered as the dissociation constant [13–17]. The fluorescence change observed when all ligand-binding sites are occupied (ΔF_{max}) is obtained at saturating concentrations of the ligand. When it is not possible to saturate acceptor with ligand under the conditions of assay owing to factors such as a large inner filter effect at high ligand concentration, ΔF_{max} may be obtained by extrapolation procedures. ΔF_{max} can also be obtained by titrating t solution of fixed total ligand concentration with an increasing concentration of protein.

In systems where the total concentration of ligand ($[L_t]$) is much bigger than the total protein concentration, ($[P_t]$), the free ligand concentration, ($[L_f]$), can be compared with the total ligand concentration. Under such circumstances, F_{max} can be obtained from a conventional double reciprocal plot of $1/\Delta F$ versus $1/[L_t]$ by extrapolating to infinite concentrations of ligand. If the bound ligand is significantly

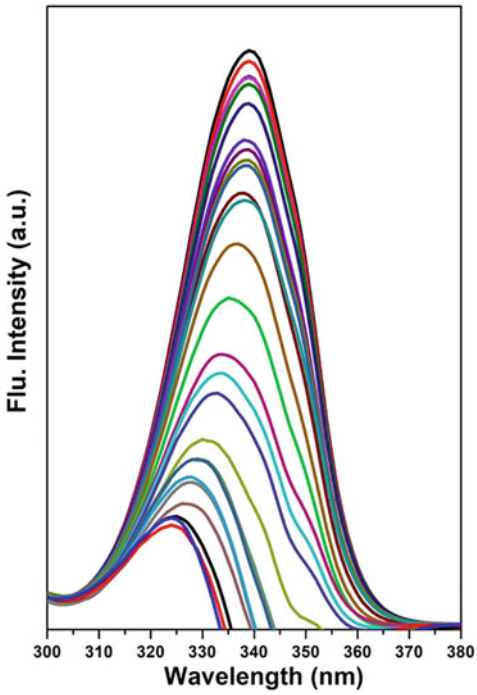

Fig. 3.1 Change in fluorescence intensity of protein upon ligand binding

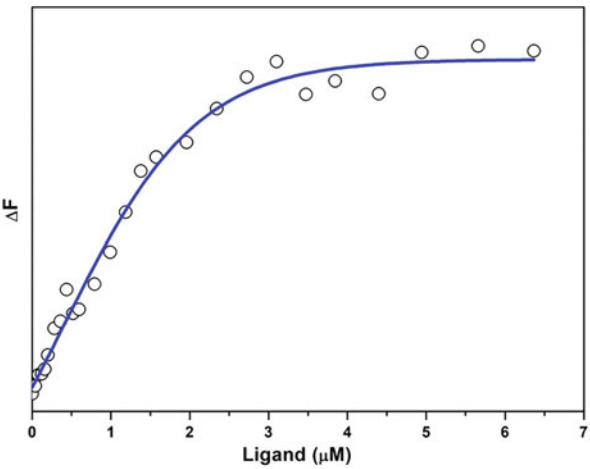

Fig. 3.2 A Plot of ligand concentration versus the change in fluorescence depicts the binding interactions between the protein and ligand

comparable to the total concentration of the ligand, this method may result in the wrong estimation of $\Delta F_{max,}$ as a linear relationship will not exist between $1/\Delta F$ and $1/[L_t]$ under such conditions. The ratio $\Delta F/\Delta F_{max}$ matches the fractional possession of total protein-binding sites (α) by ligand. The association constants related to the interaction can be obtained from conventional double reciprocal plots (Chipman Analysis) [18] or Scatchard plots [19].

3.2.1.1 Chipman Analysis

Double reciprocal plot or the plot of $1/\Delta F$ versus $1/[L_t]$, where ΔF is change in fluorescence intensity of the protein at a given ligand concentration during the titration, yields a straight line (Fig. 3.3) [18, 20]. From the ordinate of the plot, $F_{\alpha,}$ the fluorescence intensity when all the ligand molecules are bound to the protein was calculated. The binding constant, K_a, can be obtained from the abscissa of the plot of log $\{\Delta F/ (F_c - F_\alpha)\}$ versus log $[L_f]$.

According to Chipman et al. (1967):

$$\text{Log}\ \{\Delta F/(F_c - F_\alpha)\} = \log K_a + \log\ [L_f] \tag{3.2}$$

where $[L_t]$ is the total ligand concentration in solution, $[L_f]$ is the concentration of free ligand (without bound protein), and $[P_t]$ is the total concentration of protein (Fig. 3.4).

$$[L_f] = [L_t] - P_t[\Delta F/\Delta F_\alpha] \tag{3.3}$$

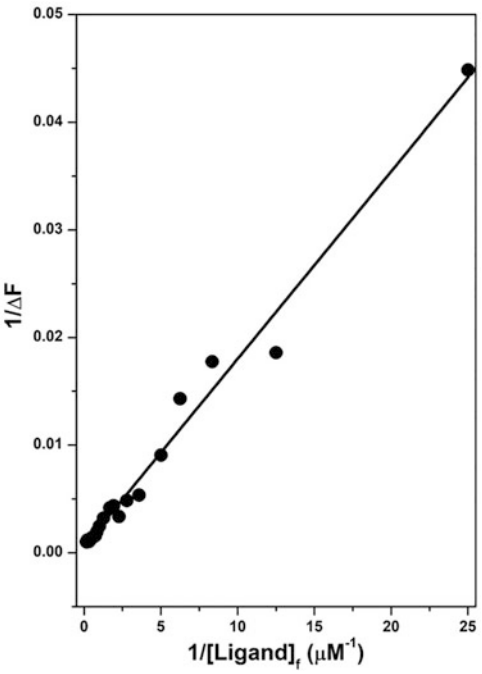

Fig. 3.3 The double reciprocal plot of $1/[\Delta F]$ versus 1/[Ligand]

3.2.1.2 Scatchard Plot Analysis

For the Scatchard plot analysis of fluorescence titrations, protein quantity is maintained at very low concentrations such that $[L]_{bound} << [L]_{total}$, and for further investigation of titration data, $[L]_{total}$ could be used as a good estimate for free ligand concentration. Plot of $\{F_r/[L]\}$ versus F_r, where F_r is ratio of corrected fluorescence intensity (F_{corr}) [$F_{corr} = F_{obs}$ antilog $[(OD_{ex} + OD_{em})/2]$ and maximum fluorescence intensity (F_{max}) of the binding data, is used to analyze the binding (Fig. 3.2b). Association constant K_a and the number of binding sites are obtained respectively from the slope and x intercept of the Scatchard plot (Fig. 3.5) [20]. A typically reversible binding for the protein "P" and ligand "L" can be expressed as

$$P + nL \leftrightarrow PLn,$$

where n represents the total number of binding sites available on the protein for the ligand of interest, and PL_n denotes the protein–ligand macromolecular complex. The average number of ligand molecules "r" that can bind to the protein molecule at any given concentration of $[P]$ and $[L]$ is given as:

$$r = [PL_n]/[P] \tag{3.4}$$

While the Scatchard equation is expressed as:

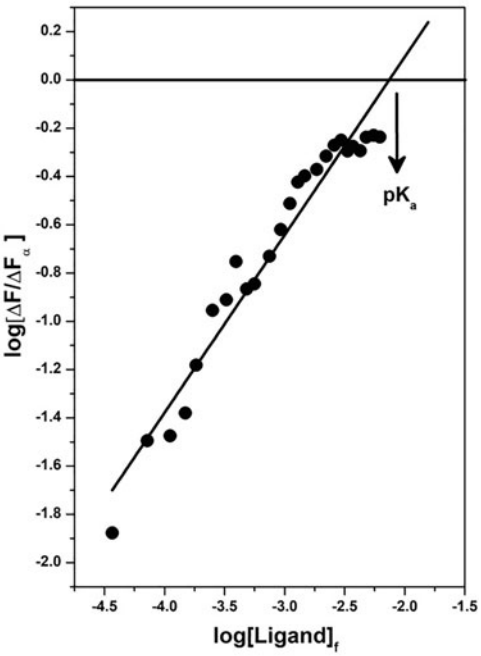

Fig. 3.4 A linear plot representing the Chipman analysis to follow the binding of ligand to the protein and estimate the associate constant (K_a)

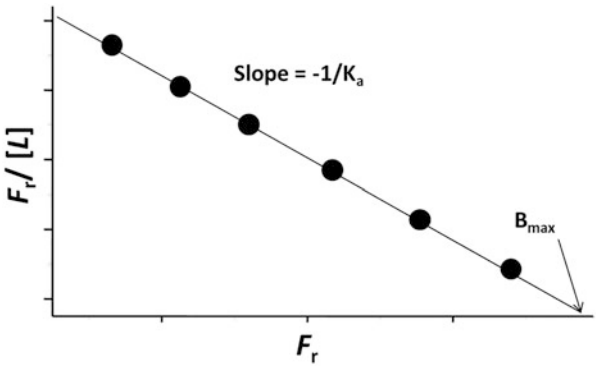

Fig. 3.5 Representation of a Scatchard plot of $F_r/[L]$versus F_r

$$r/[L] = nK_a - rK_a \tag{3.5}$$

A plot of $r/[L]$ versus r provides a slope of $-K_a$, and K_a represents the association (affinity) constant of the protein for the specific ligand. A deviation from linearity is observed if the interaction involves multiple binding sites on the protein (positive or negative cooperativity).

3.2.1.3 Quantification Using Labeled Ligand

For quantification of binding reactions using fluorescent ligand, ligand (L) containing a fluorophore should be capable of forming a complex (ASL) without interfering with the binding interactions of protein A with compound S. The reaction may be shown as

$$\mathrm{A} + \mathrm{S} \overset{K}{\rightleftarrows} \mathrm{AS}$$

$$\mathrm{AS} + L \overset{K_L}{\rightleftarrows} \mathrm{AS}L$$

While interacting with the complex AS, the spectroscopic properties of the ligand L alter substantially. Supposing L is present in large excess comparative to the complex, $[\mathrm{AS}L] = K_L[L][\mathrm{AS}] \approx K_L[L]_{\mathrm{tot}}[\mathrm{AS}] = K_L[L]_{\mathrm{tot}}K[\mathrm{A}][\mathrm{S}] = K_{\mathrm{obs}}[\mathrm{A}][\mathrm{S}]$. The observed binding constant (K_{obs}) can be obtained by tracking the amount of ASL at several concentrations of S (with the concentration of A fixed). The binding constant ($K_{\mathrm{d}} = 1/K$) can be estimated by knowing the values of K_L and $[L]_{\mathrm{tot}}$ [21–23].

3.2.1.4 Correction for Inner Filter Effect

Because of the absorption of the incident and emitted light passing through the cell, the recorded fluorescence intensity of the sample for which the emission is detected usually varies disproportionally to sample concentration, and this process is called the inner filter effect. In other words, the inner filter effect is caused by the reabsorption of emitted light by the quencher.

Inner filter effect can be calculated by the equation:

$$F_{\mathrm{corr}} = F_{\mathrm{obs}}\mathrm{Antilog}\left[(\mathrm{OD}_{\mathrm{ex}} + \mathrm{OD}_{\mathrm{em}})/2\right] \tag{3.6}$$

where F_{corr} and F_{obs} are the corresponding corrected and observed fluorescence intensities, and $\mathrm{OD}_{\mathrm{ex}}$ and $\mathrm{OD}_{\mathrm{em}}$ are the respective absorption intensities of the sample at the excitation wavelength and emission wavelength [22].

To reduce the inner filter effect,

- reduce the concentration of the sample. To get good results, optical density is kept preferably <0.1.
- excitation at 10–50 nm below the absorption maximum is recommended to avoid secondary inner filter effects.
- Decrease the chosen path length. To reduce the path length and consecutively the absorbance of the sample, choose a small-capacity cuvette or a triangular cuvette or move the cuvette holder such that the cuvette area measured is near the corner.

3.2.1.5 Applications

Steady-state fluorescence spectroscopy is useful for studying protein–substrate interactions, protein–nucleic acid interactions, protein–nucleotide interactions,

protein–protein interactions, etc. The binding of drugs with carrier proteins is essential for the transport and metabolism of drugs. The microenvironment and architecture experienced by the ligand is determined largely by the folding/unfolding and/or transformation of protein structure during the interaction. In drug development for example, information about the binding site is very crucial, and this information is provided by spectroscopic properties of ligand housed in the microenvironment of proteins like serum proteins, which in turn will reflect the immediate surroundings of the molecule inside the target proteins [24–28]. Changes in fluorescence properties associated with protein–nucleotide interactions may be used as sensors for enzymatic activities or as probes for screening inhibitors/natural substrates [29–31]. A 2.5-fold increase in fluorescence is observed upon binding of Mant-ATP, a nucleotide analog to the cyclin-dependent kinase (Cdk2) that allows one to determine the dissociation constant [32, 33]. Fluorescently labeled oligonucleotides were used to investigate the mechanism of several DNA or RNA polymerases as well as to monitor the binding of regulatory proteins [34].

A combination of steady-state transient kinetic, and FRET single-molecule assay using dyes attached to the enzyme or its different partners helped in unraveling the structure and mechanism of the reverse transcriptase (RT) of HIV (human immunodeficiency virus), a key enzyme in the virus replication cycle that catalyzes a chain of reactions to convert the single-stranded HIV RNA genome into a double-stranded DNA for further integration in the host cell genome. The large change in dye fluorescence upon binding of primer/template oligonucleotide to RT was used to follow this interaction. These investigations have shown that catalysis of RT is dependent on the binding orientation of the substrate, which adopts opposite conformations for DNA and RNA duplexes [35–38].

Protein/protein interaction studies provide better a understanding of the different parameters that rule the association of protein complexes. Analyses of these parameters enable the development of shorter peptides with similar interaction properties as well as in the design of novel inhibitors of specific protein/protein interactions as well as biosensors of protein complexes [39–42]. Information obtained using fluorescence spectroscopy regarding the structure, organization, and dynamics of membrane proteins could be crucial for a better understanding of their role in health and diseases, as large a number of cellular functions are mediated through membrane proteins, which also play a vital role in pathogenicity [43].

3.2.2 Fluorescence Analysis of Protein–Lipid Interaction

Tryptophan (Trp) fluorescence measurements are one of the important methods used to investigate membrane interaction of human Glycolipid transfer protein (GLTP) (Fig. 3.6a). GLTP is excited at 295 nm, and emission spectra are measured from 310 to 420 nm. To avoid inner filter effects, protein concentration should be maintained at $A_{295} < 0.1$ [44]. While investigating the membrane interactions, the variation in emission signals from the Trp of GLTP (1 μM) is monitored with the addition of small aliquots of the phosphatidylcholine (PC) vesicles with/without

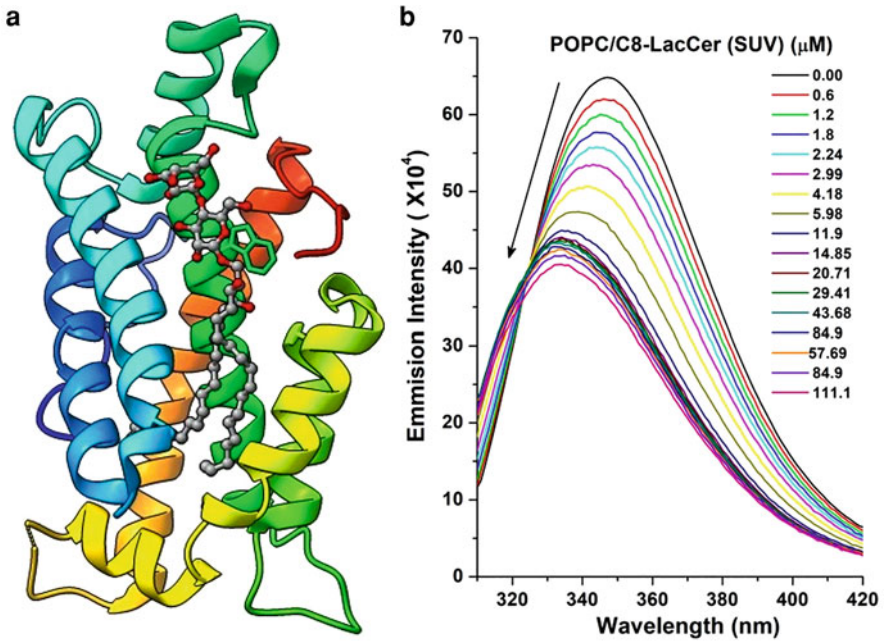

Fig. 3.6 (**a**) Model depicting the binding of GLTP with glycolipid, lactosylceramide (LacCer), and the probe residue (Trp96) is shown in stick model, and ligand is represented as ball and stick. (**b**) Decrease in Trp fluorescence of GLTP due to addition of POPC lipids vesicles having LacCer aliquots

glycolipid (20 mol%) (Fig. 3.6b). To assess the direct binding of glycolipid to GLTP, micro addition of glycolipids dissolved in ethanol can be followed [44, 45]. Measurements were accomplished with constant stirring along with the addition of 0.1 mM GSL to 1 μM of protein.

3.2.2.1 Binding (Partitioning) Coefficient Analysis

The total number of binding sites (α) occupied by glycolipids can be determined by the following Eq. (3.7):

$$\alpha = (F - F_o)/F_{max} \tag{3.7}$$

where F_o and F are the emission intensities of the Trp residues in GLTP (in the absence and presence of glycolipid, respectively). The emission intensity of the completely saturated GLTP (at excess glycolipid) is F_{max} [46, 47]. By plotting a graph $1/(F - F_o)$ versus $1/L$, F_{max} can be determined (extrapolating $1/L = 0$, where L = total glycolipid concentration). The maximum change in the protein fluorescence (ΔF_m) is observed at saturating concentrations of glycolipid, and it is estimated by plotting $1/L$ against $1/\Delta F$. The following relationship was used to calculate the concentration of bound glycolipid to the protein:

$$[\text{Bound Lipid}] = \text{Concentration of Protein} \times \Delta F/\Delta F_{\text{m}} \tag{3.8}$$

The concentration of free lipid is calculated as:

$$[\text{Free lipid}] = [\text{Total lipid}] - [\text{Bound lipid}] \tag{3.9}$$

K_{d} values can be determined by nonlinear least-squares (NLLSQ) fit of the plot of bound lipid versus free lipid.

Spectral data of fluorescence titration by the ethanol injection method were analyzed according to:

$$\varepsilon - 1 = (\varepsilon_{\text{b}} - 1) - K_{\text{d}}(\varepsilon - 1)/mn \tag{3.10}$$

where K_{d} is the dissociation constant of lipid–protein complex, m is the concentration of lipid, and n is the number of binding sites of lipid. The quantity ε is the spectral parameter relative value (peak emission wavelength, λ_{max}, or intensity, I) associated with lipid binding to GLTP at a concentration of lipid "m". Thus, ε can symbolize either I/I_{o} or $(\lambda_{\text{max}})_{\text{o}}/\lambda_{\text{max}}$, where the subscript "o" refers to the values in the absence of lipid. The parameter ε_{b} represents the spectral properties of the protein–lipid complex. As per Eq. (3.10), $\varepsilon - 1$ versus $(\varepsilon - 1)/m$ graph gives the slope as K_{d}/n, the reciprocal of the protein/lipid association constant.

3.3 Fluorescence Quenching Analysis

Fluorescence quenching refers to any process that involves a variety of molecular interactions that lead to a reduction in fluorescence intensity. The interactions can be energy transfer, ground state complex formation, excited state reactions, molecular collisions, etc.

Quenching is broadly classified under two categories: static and dynamic quenching. Dynamic quenching involves a collision between two molecules with fluorophore losing energy as kinetic energy. In other words, dynamic quenching occurs when the fluorophore and another molecule diffuse in solution and collide with each other. Each collisional events lead to the transfer of excitation energy to the quencher molecule. Molecules do not form complex in this case.

Static quenching occurs when two molecules interact with each other to form a complex (Fig. 3.7). The interaction between the two molecules can be monitored by means of variation in the intrinsic fluorescence of aromatic amino acids or using extrinsic fluorophores such as ANS. Changes in fluorescence parameters can be used to follow the interaction [48–50]. This technique has been employed for various applications including pathogen sensing, chemosensing, heavy metal detection, imaging, etc. The extent of quenching can be quantitatively estimated using the Stern–Volmer equation.

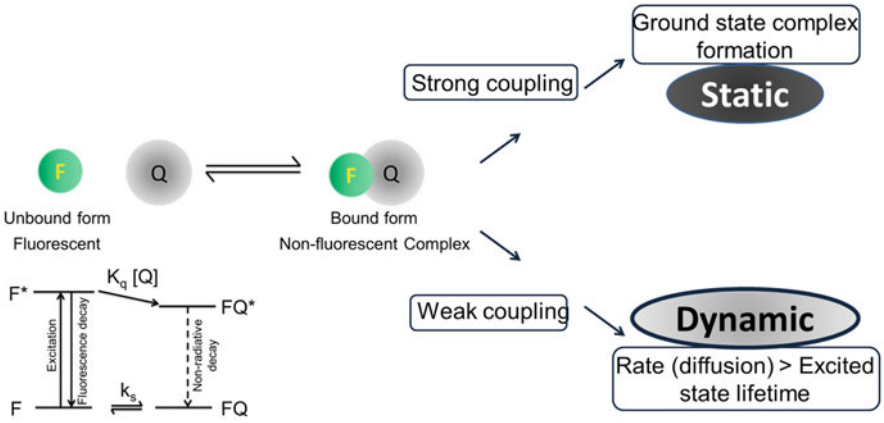

Fig. 3.7 Schematic illustration of fluorescence quenching: static and dynamic

3.3.1 Collisional Quenching: The Stern–Volmer Plot

The relationship between the ratio of fluorescence intensity in the absence and presence of quencher and the concentration of quencher is known as the Stern–Volmer equation.

$$F_o/F_c = 1 + K_{SV}[Q] \tag{3.11}$$

where F_o and F_c are the respective fluorescence intensities in the absence and presence of the quencher, K_{SV} is the Stern–Volmer (SV) quenching constant, and $[Q]$ is the concentration of the quencher.

A linear Stern–Volmer plot suggests a single class of fluorophores available to the quencher equally. SV plots often show deviation from linearity because of a variety of factors such as heterogeneity in fluorophore excited state, the mixture of quenching mechanisms, and deviation from ideal behavior.

Static quenching will dominate at higher concentrations and diffusional quenching at lower. In the case of static quenching, the slope of the graph decreases, while for dynamic quenching, it rapidly increases with temperature. In the former case, the complex formation is inhibited with an increases in temperature, while in the latter one, the number of collisions increases with temperature. The shape and position of the fluorescence spectrum change with protein concentration for static quenching, while during dynamic quenching, fluorescence intensity decreases without change in shape and position of the spectrum. Linear SV plots are obtained for dynamic quenching. An upward curvature is explained in terms of both static and dynamic quenching. A downward curvature may be indicative of static quenching and may be attributed to fractional accessibility of fluorophore to the quencher. In such situations, modified Stern–Volmer plots are used for analyzing the process.

Modified Stern–Volmer equation is expressed as:

$$F_o/\Delta F = f_a^{-1} + (K_a f_a)^{-1}[Q]^{-1} \tag{3.12}$$

where f_a is the portion of fluorophore sites available to the quencher, and K_a is the Stern–Volmer quenching constant. When there is an explicit interaction between protein and the quencher during complex formation, the modified Stern–Volmer plot displays linearity.

The position of the fluorophore within the protein determines its accessibility to the solvent and subsequently to the quencher. For instance, Trp present at the surface residues will have better accessibility to the solvent as compared to the buried ones. Hydrophobic regions of proteins are not freely accessible even to water-soluble quenchers, like iodide and acrylamide. The quenching constant is intensely influenced by the emission maximum. Studies reveal that a red-shifted is observed when the tryptophan residues of proteins are almost completely accessible to acrylamide quenching and blue-shifted when the tryptophan residues remain largely inaccessible to quenching by acrylamide. Being polar molecules, acrylamide and iodide cannot readily enter into the nonpolar regions of proteins. Small nonpolar oxygen molecules on the other hand can freely enter.

In the recent past, emitting semiconductor quantum dots along with quenchers were employed for detecting biologically significant molecules [51, 52]. But their applications were limited by their poor biodegradability and potential toxicity. Recently, fluorescence emission from graphene quantum dots was quenched by novel MnO_2 nanoflowers and has been demonstrated for the detection of intracellular glutathione [53]. This method follows a "fluorescence turn-on" mechanism for its detection (Fig. 3.8). The interaction between the fluorophore and the quencher was electrostatic. In the presence of glutathione, the nanoprobe MnO_2-GQDs formed by the adsorption of MnO_2 degrade to release Mn^{2+} and highly fluorescent free GQDs. This method was reported to be highly specific and sensitive for glutathione with a detection limit of 2.8 μM. This method can be extended for cellular imaging to detect GSH.

For the past few decades, ethidium bromide has been used as a luminescent probe to investigate the binding of small molecules or drugs to nucleic acids [54]. It is known that neither ethidium bromide nor the nucleic acids are fluorescent as such, but when they form a complex with each other, they become fluorescent. But ethidium bromide being a carcinogen, its use is limited as a probe. Recently, nanoceria particles were reported to form bionanoconjugates with nucleic acid

Fig. 3.8 Quenching of fluorescence from graphene quantum dots by manganese dioxide nanoflowers follows a fluorescence turn-on mechanism in the detection of intracellular glutathione

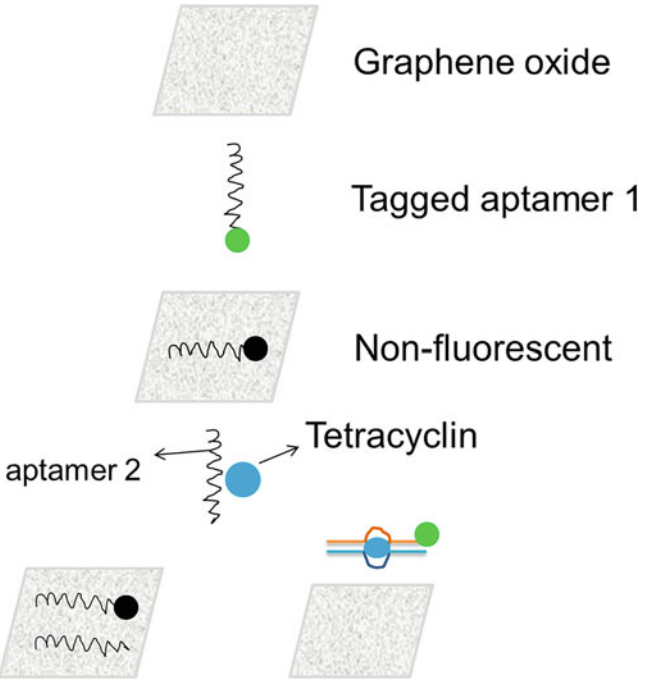

Fig. 3.9 Schematic represents the principle involved in the detection of tetracycline by fluorescence turn-on aptasensing method with graphene oxide and fluorophore-tagged aptamer

bases and were utilized as molecular nanoprobes, for the single-step investigation of oligonucleotides [55]. This method has a detection limit of 0.12 nM. This method can find a wide range of applications [56] in diagnostics, biosensors and chemosensors, gene expression analysis, cellular imaging, and forensic analysis.

The fluorescence turn-on aptasensing method has been proposed for the detection of tetracycline in animal-derived food (Fig. 3.9). Tetracycline being reported as an allergen to humans, its use in excess leaves out its residues in animal-derived food products [57]. In this method, a tetracycline binding RNA aptamer that is linked to a fluorophore is employed for detection. The tagged aptamer becomes fluorescent only upon detecting tetracycline, as this disrupts the π–π stacking between the graphene oxide (GO) surface and the tagged aptamer. This leads to the inhibition of quenching caused by energy transfer from the fluorophore to the GO surface. The method developed was highly efficient to detect tetracycline selectively and sensitively in animal-derived food products. Though several other methods including HPLC, ELISA, and LC-MS are available, they are complicated and require skilled labor.

3.4 Red-Edge Excitation Shift (REES) Analysis

It is known that the emission spectra are always independent of the excitation wavelength when the solvent relaxation times are much faster than the life time of the excited electronic state. But this is not true when the spectra are recorded in a polar environment with considerably high viscosity. In an equilibrium condition, a fraction of the ground state molecules are likely to have the same solvation sphere as the relaxed excited state. Excitation of such low-energy molecules leads to an emission spectrum that is more red-shifted. Such phenomenon is known as red-edge excitation spectrum or red-edge excitation shift (REES). REES is an optical phenomenon that can be utilized to obtain unique information on molecular conformations and the associated equilibrium. In this technique, the more stable fluorophores are excited resulting in a red shift in the maximum of the emission intensity. This phenomenon helps to identify the fluorescent conformers with varying solvation spheres and biomolecular binding interactions in the ground and excited states. This effect is due to a change in dipole moment which further induces a change in the extent of solvation at different electronic levels. Higher the solvation, longer will be the life time in that particular state than that of the environmental relaxation which results in an emission maximum independent of the excitation wavelength. In this method by following photoselection, it is possible to identify fluorophores in different solvation environments especially at the red edge of the excitation spectra that are in equilibrium. Experimentally, one observes a red shift in the emission maximum with respect to the excitation wavelength. In the case of proteins, the intrinsic fluorescence from the tryptophan and/or tyrosine varies depending on the proportions of the folded, molten globule, or unfolded states [58, 59]. Using this REES method, a novel and structurally unique lipid-binding motif has been identified and investigated in human glycolipid transfer protein [45].

There are several reports wherein the selective excitation of species in a complex environment to instigate its chemical reaction in a controlled manner was studied extensively. Similar studies were carried out for benzophenone and its coordination with phenol via hydrogen bonding in a polar aprotic solvent [60]. Antimicrobial peptides have high selectivity toward bacterial targets in various host cells and have restricted bacterial resistance. The role of pH on the activity and biophysical properties of one such peptide C18G was investigated by red-edge excitation spectroscopy (REES). It was shown that clear pH dependence toward aggregation was observed [61].

In another study, the binding interactions of malathion with human serum albumin in the presence of silver nanoparticles were investigated using various optical techniques including fluorescence quenching, fluorescence resonance energy transfer (FRET), circular dichroism, red-edge excitation shift (REES), synchronous fluorescence, and three-dimensional fluorescence spectroscopy. The results of synchronous fluorescence spectroscopy and REES indicated the changes in the microenvironment of the fluorophore [62].

3.5 Synchronous Spectroscopy

Synchronous spectroscopy is a technique that has been used for the investigation of multicomponent systems. This method is considered as a simple optical method with minimum light scattering compared to conventional steady-state fluorescence emission methods, where difficulty with the analyses of impure or mixture of samples exists. Synchronous fluorescence spectroscopy was first developed by Lloyd. Here, both the emission and excitation monochromators are scanned simultaneously during measurement to get the synchronous spectrum. The advantages include spectral simplification, bandwidth narrowing, minimized scattering, and enhanced resolution. It also provides high selectivity and sensitivity in analytical measurements of complex samples [63].

There are two types of synchronous fluorescence spectra: constant wavelength or constant energy and variable angle (Fig. 3.10). The choice of type selection depends on the flexibility and selectivity of the measurements to be made. From the above spectrum, it is possible to generate an isopotential trajectory by connecting the points of equal intensity.

Synchronous spectroscopy has been in the application of determining polycyclic aromatic hydrocarbons, benzopyrenes, benzofluoranthene, anthracene, etc. in

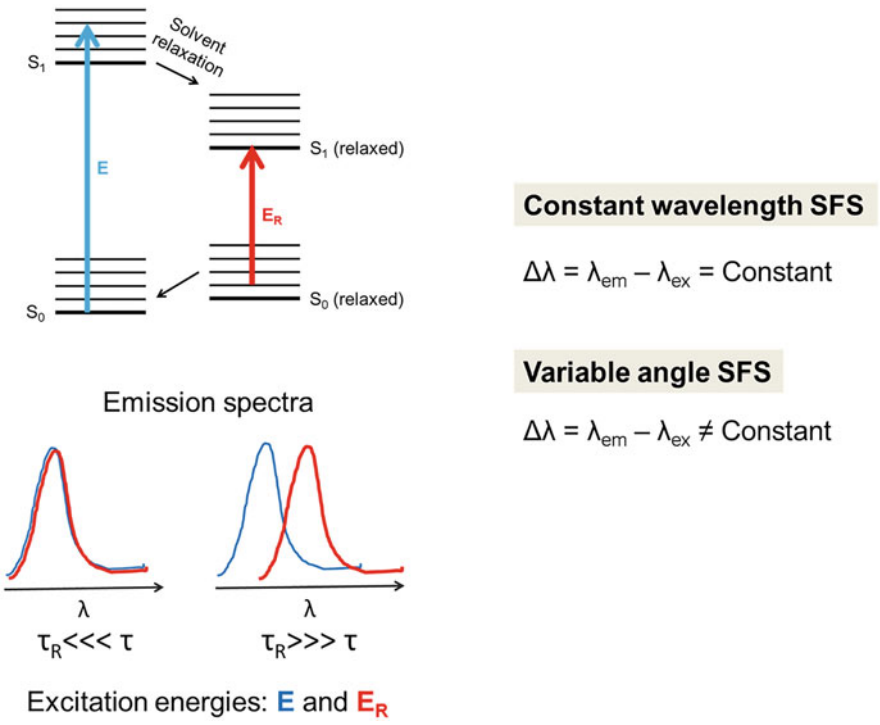

Fig. 3.10 Schematic representing the principle of synchronous fluorescence spectroscopy

foodstuffs. Moreover, these approaches are rapid, cost-effective, and efficient as an analytical tool for rapid screening of metabolized products and by-products in a large number of human samples [64] like blood, feces, and saliva. Overall, the combination of these approaches along with other techniques, such as derivative and/or low-temperature techniques and chemometrics, has shown potential performances in real-time applications. These techniques also serve as potential tools for clinical analysis and food safety evaluation [65–67].

The potential of fluorescence spectroscopy is not limited to the above discussions. With the emergence of new diseases and more virulent pathogens, investigations on novel therapeutics and diagnostic methods need to be intensified. Thermally activated delayed fluorescence (being employed for imaging applications) and circularly polarized emission (being employed as a probing tool to monitor luminescent chiral molecular systems and in particular the biological systems) are some of the advanced optical methods optical techniques that are still in their preliminary stage of development. There is still a lot more to be explored for implications of fluorescence-assisted techniques for the advent of many probing devices.

References

1. Lakowicz JR (ed) (2013) Principles of fluorescence spectroscopy. Springer Science and Business media, Berlin
2. Demchenko AP, Lakowicz JR (eds) (1991) Topics in fluorescence spectroscopy: biochemical applications. Plenum, New York, pp 65–112
3. Lakowicz JR (2002) Principles of fluorescence spectroscopy, 2nd edn. Kluwer Academics/Plenum, NewYork, pp 445–486
4. Saxena A, Udgaonkar JB, Krishnamoorthy G (2005) Protein dynamics and protein folding dynamics revealed by time-resolved fluorescence. In: Hof M, Hutterer R, Fidler V (eds) Fluorescence spectroscopy in biology, vol 3. Springer, Berlin, Heidelberg, pp 163–179
5. Eftink MR (1994) The use of fluorescence methods to monitor unfolding transitions in proteins. Biophys J 66:482–501
6. Chen Y, Barkley MD (1998) Toward understanding tryptophan fluorescence in proteins. Biochemistry 37(28):9976–9982
7. Demchenko AP, Mély Y, Duportail G, Klymchenko AS (2009) Monitoring biophysical properties of lipid membranes by environment-sensitive fluorescent probes. Biophys J 96(9):3461–3470
8. Martin MM, Lindqvist L (1975) The pH dependence of fluorescein fluorescence. J Lumin 10:381–390
9. Ma LY, Wang HY, Xie H, Xu LX (2004) A long lifetime chemical sensor: study on fluorescence property of fluorescein isothiocyanate and preparation of pH chemical sensor. Spectrochim Acta A Mol Biomol Spectrosc 60(89):1865–1872
10. Varlan A, Hillebrand M (2010) Study on the interaction of 2-carboxyphenoxathiine with bovine serum albumin and human serum albumin by fluorescence spectroscopy and circular dichroism. Rev Roum Chim 55:69–77
11. Khan SN, Islam B, Khan AU (2007) Probing midazolam interaction with human serum albumin and its effect on structural state of proteins. Int J Integr Biol 1(2):102–112
12. Alarcón E, Edwards AM, Aspée A, Borsarelli CD, Lissi EA (2009) Photophysics and photochemistry of Rose Bengal bound to human serum albumin. Photochem Photobiol Sci 8:933–943

13. Weljie AM, Vogel HJ (2002) Steady-state fluorescence spectroscopy. Methods Mol Biol 173: 75–87
14. Ward LD (1985) Measurement of ligand binding to proteins by fluorescence spectroscopy. Methods Enzymol 117:400–414
15. Mocz G, Ross JA (2013) Fluorescence techniques in analysis of protein-ligand interactions. Methods Mol Biol 1008:169–210
16. Yammine A, Gao J, Kwan AH (2019) Tryptophan fluorescence quenching assays for measuring protein-ligand binding affinities: principles and a practical guide. BioProtocol 9(11):e3253
17. Williams MA, Daviter T (eds) (2013) Protein-ligand interactions: methods and applications, methods in molecular biology. Springer Science Business Media, New York, p 1008
18. Chipman DM, Grisaro V, Sharon N (1967) The binding of oligosaccharides containing N-acetylglucosamine and N-acetylmuramic acid to lysozyme. J Biol Chem 242:4388–4394
19. Roberts DD, Goldstein IJ (1982) Lectin from Lima beans (Phaseolus lunatus). J Biol Chem 257: 11274–11277
20. Komath SS, Kenoth R, Swamy MJ (2001) Thermodynamic analysis of saccharide binding to snake gourd (Trichosanthesanguina) seed lectin fluorescence and absorption spectroscopic studies. Eur J Biochem 268:111–119
21. Khan MI, Mazumder T, Pain D, Gaur N, Surolia A (1981) Binding of 4-methylumbelliferyl b-d-galactopyranoside to Momordica charantia lectin. Eur J Biochem 113:471–476
22. Bessler W, Shafer J, Goldstein IJ (1974) Spectroscopic study of the carbohydrate binding site of con a. J Biol Chem 249:2819–2822
23. Kubista M, Sjöback R, Ericsson S, Albinsson B (1994) Experimental correction for the inner-filter effect in fluorescence spectra. Analyst 119:417–419
24. Royer CA (2006) Probing protein folding and conformational transitions with fluorescence. Chem Rev 106(5):1769–1784
25. Cohen BE, McAnaney TB, Park ES, Jan YN, Boxer SG, Jan LY (2002) Probing protein electrostatics with a synthetic fluorescent amino acid. Science 296:1700–1703
26. Abou-Zied OK, Al-Shini OIK (2008) Characterization of subdomain IIA binding site of human serum albumin in its native, unfolded, and refolded states using small molecular probes. J Am Chem Soc 130(32):10793–10801
27. Er JC, Vendrell M, Tang MK, Zhai D, Chang YT (2003) Fluorescent dye cocktail for multiplex drug-site mapping on human serum albumin. ACS Comb Sci 15(9):452–457
28. Yamasaki K, Chuang VTG, Maruyama T, Otagiri M (2013) Albumin–drug interaction and its clinical implication. Biochim Biophys Acta 1830:5435–5443
29. Bagshaw C (2001) ATP analogues at a glance. J Cell Sci 114:459–460
30. Jameson DM, Eccleston JF (1997) Fluorescent nucleotide analogs: synthesis and applications. Methods Enzymol 278:363–390
31. Weisbrod SH, Marx A (2008) Novel strategies for the site-specific covalent labelling of nucleic acids. Chem Commun (Camb) 44:5675–5685
32. Morris MC, Gondeau C, Tainer JA, Divita G (2002) Kinetic mechanism of activation of the Cdk2/cyclin a complex. Key role of the C-lobe of the Cdk. J Biol Chem 277(26):23847–23853
33. Heitz F, Morris MC, Fesquet D, Cavadore JC, Dorée M, Divita G (1997) Interactions of cyclins with cyclin-dependent kinases: a common interactive mechanism. Biochemistry 36(16): 4995–5003
34. Creighton TE (2010) The biophysical chemistry of nucleic acids and proteins. Helvetian Press, Eastbourne
35. Divita G, Müller BU, Immendörfer U, Gautel M, Rittinger K, Restle T, Goody RS (1993) Kinetics of interaction of HIV reverse transcriptase with primer/template. Biochemistry 32(31): 7966–7971
36. Liu S, Harada BT, Miller JT, Le Grice SFJ, Zhuang X (2010) Initiation complex dynamics direct the transitions between distinct phases of early HIV reverse transcription. Nat Struct Mol Biol 17:1453–1460

37. Abbondanzieri EA, Bokinsky G, Rausch JW, Zhang JX, Le Grice SFJ, Zhuang X (2008) Dynamic binding orientations direct activity of HIV reverse transcriptase. Nature 453(7192): 184–189
38. Agopian A, Depollier J, Lionne C, Divita G (2007) Trp24 and Phe61 are essential for accurate association of HIV-1 reverse transcriptase with primer/template. J Mol Biol 373(1):127–140
39. Kurzawa L, Morris MC (2010) Cell-cycle markers and biosensors. Chem Biochem 11(8): 1037–1047
40. Kurzawa L, Pellerano M, Coppolani JB, Morris MC (2011) Fluorescent peptide biosensor for probing the relative abundance of cyclin-dependent kinases in living cells. PLoS One 6(10): e26555
41. Gondeau C, Gerbal-Chaloin S, Bello P, Aldrian-Herrada G, Morris MC, Divita G (2005) Design of a novel class of peptide inhibitors of cyclin-dependent kinase/cyclin activation. J Biol Chem 280(14):13793–13800
42. Pommier Y, Cherfils J (2005) Interfacial inhibition of macromolecular interactions: nature's paradigm for drug discovery. Trends Pharmacol Sci 26(3):138–145
43. Bianchi G, Carafoli E, Scarpa A (1986) Membrane pathology. Ann N Y Acad Sci 488:1–153
44. Kamlekar RK, Gao Y, Kenoth R, Molotkovsky JG, Prendergast FG, Malinina L, Patel DJ, Wessels WS, Venyaminov SY, Brown RE (2010) Human GLTP: three distinct functions for the three Tryptophans in a novel peripheral amphitropic fold. Biophys J 99:2626–2635
45. Kenoth R, Zou X, Simanshu DK, Pike HM, Malinina L, Patel DJ, Brown RE, Kamlekar RK (2018) Functional evaluation of intrinsic Tryptophans in glycolipid binding and membrane interaction by HETC2, a fungal glycolipid transfer protein. Biochim Biophys Acta Biomembr 1860(5):1069–1076
46. Santra MK, Panda D (2003) Detection of an intermediate during unfolding of bacterial cell division protein FtsZ: loss of functional properties precedes the global unfolding of FtsZ. J Biol Chem 278:21336–21343
47. Srivastava R, Ratheesh A, Gude RK, Rao KVK, Panda D, Subrahmanyam G (2005) Resveratrol inhibits type II phosphatidylinositol 4-kinase: a key component in pathways of phopsphoinositide turnover. Biochem Pharmacol 70:1048–1055
48. Eftink MR, Ghiron CA (1981) Fluorescence quenching studies with proteins. Anal Biochem 114:199–227
49. Eftink MR, Ghiron CA (1976) Exposure of tryptophyl residues in proteins. Quantitative determination by fluorescence quenching studies. Biochemistry 15:672–680
50. Eftink MR, Ghiron CA (1976) Fluorescence quenching of indole and model micelle systems. J Phys Chem 80:486–493
51. Clift MJ, Stone V (2012) Quantum dots: an insight and perspective of their biological interaction and how this relates to their relevance for clinical use. Theranostics 2:668–680
52. Holzinger M, Le Goff A, Cosnier S (2014) Nanomaterials for biosensing applications: a review. Front Chem 2:63
53. Song ZL, Dai X, Li M, Teng H, Song Z, Xie D, Luo X (2018) Biodegradable nanoprobe based on MnO_2 nanoflowers and graphene quantum dots for near infrared fluorescence imaging of glutathione in living cells. Mikrochim Acta 185:485
54. Kiran T, Vasavi CS, Munusami P, Pathak M, Balamurali MM (2017) Evaluation of DNA/protein interactions and cytotoxic studies of copper (II) complexes incorporated with N, N donor ligands and terpyridine ligand. Int J Biol Macromol 95:1254–1266
55. Bulbul G, Hayat A, Mustafa F, Andreescu S (2018) DNA assay based on Nanoceria as fluorescence quenchers (NanoCeracQ DNA assay). Sci Rep 8:2426
56. Liu B, Liu J (2015) Comprehensive screen of metal oxide nanoparticles for DNA adsorption, fluorescence quenching, and anion discrimination. ACS Appl Mater Interfaces 7:24833–24838
57. Zhang L, Wang J, Deng J, Wang S (2020) A novel fluorescent "turn-on" aptasensor based on nitrogen-doped graphene quantum dots and hexagonal cobalt oxyhydroxide nanoflakes to detect tetracycline. Anal Bioanal Chem 412:1343–1351
58. Patra SK, Pal MK (1997) Red edge excitation shift emission spectroscopic investigation of serum albumins and serum albumin-bilirubin complexes. Sectrochim Acta Pt A Mol Biomol Spectrosc 53A(10):1609–1614

59. Chattopadhyay A, Haldar S (2014) Dynamic insight into protein structure utilizing red edge excitation shift. Acc Chem Res 47:12–19
60. Venkatraman RK, Orr-Ewing AJ (2019) Photochemistry of benzophenone in solution: a tale of two different solvent environments. J Am Chem Soc 141:15222–15229
61. Hitchner MA, Santiago-Ortiz LE, Necelis MR, Shirley DJ, Palmer TJ, Tarnawsky KE, Vaden TD, Caputo GA (2019) Activity and characterization of a pH-sensitive antimicrobial peptide. Biochim Biophys Acta Biomembr 1861:182984
62. Baghaee PT, Divsalar A, Jamshikhan CJ, Donya A (2019) Human serum albumin–malathion complex study in the presence of silver nanoparticles at different sizes by multi spectroscopic techniques. J Biomol Struct Dyn 37:2254–2264
63. Rubio S, Gomez-Hens A, Valcarcel M (1986) Analytical applications of synchronous fluorescence spectroscopy. Talanta 33:633–640
64. Lecrenier MC, Baeten V, Taira A, Abbas O (2018) Synchronous fluorescence spectroscopy for detecting blood meal and blood products. Talanta 189:166–173
65. Dankowska A, Malecka M, Kowalewski W (2015) Detection of plant oil addition to cheese by synchronous fluorescence spectroscopy. Dairy Sci Technol 95:413–424
66. Durakli VS, Ercioglu E, Boyaci IH (2017) Rapid discrimination between buffalo and cow milk and detection of adulteration of buffalo milk with cow milk using synchronous fluorescence spectroscopy in combination with multivariate methods. J Dairy Res 84(2):214–219
67. Temiz HT, Tamer U, Berkkan A, Boyaci IH (2017) Synchronous fluorescence spectroscopy for determination of tahini adulteration. Talanta 167:557–562